GW170814: ANALYSIS OF GRAVITATIONAL WAVE FROM A BINARY BLACK HOLE COALESCENCE

Margherita De Toma

8 may 2021

Abstract

This work focuses on the signal produced by the coalescence of two stellar-mass black holes observed on August 14 2017 at 10:30:43 UTC from the LIGO Livingstone detector, the LIGO Hanford and from VIRGO.
We estimated the masses m_1 and m_2 of the mergers using the match filter approach.

Contents

1 **Introduction** 1

2 **Theorical model** 1

3 **Detector** 2

4 **Data Analysis** 2
4.1 Temporal analysis 2
4.2 Detector noise analysis 3
4.3 Optimal detection filter 5

5 **Conclusions** 7

References 7

1 Introduction

General relativity becomes important for very strong gravitational fields that are the more intense the more the source object is compact. The known compact objects are white dwarfs, neutron stars and black holes. Not all the sources produce waves detectable from the instruments available at present. The transient events expected to be detectable by LIGO and Virgo are coalescence of compact binary systems and core-collapse of massive stars. Furthermore, gravitational waves emission could come from non-transient sources, such as rotational pulsars with asymmetries or from the stochastic background.
The gravitational wave detection is particularly challenging since the expected signal amplitude, that is $\lesssim 10^{-21}$, is typically lower than the noise amplitude. The sources of noise are numerous: quantum noise, seismic and newtonian noise, thermal noise. During last years, the experimental apparatus has been improved with some adjustments to reduce noise strain up to one order of magnitude.
The signal was first observed at the LIGO Livingston detector at 10:30:43 UTC, and at the LIGO Hanford and Virgo detectors with a delay of ∼8 ms and ∼14 ms, respectively (as reported in [1]).
Data are retrieved from LIGO and VIRGO Observing Run 1 (O1) and 2 (O2) from 2015 to 2017.

2 Theorical model

The Einstein equation is:

$$R_{\mu\nu} - \frac{1}{2}Rg_{\mu\nu} = \frac{8\pi G}{c^4}T_{\mu\nu}. \tag{1}$$

Assuming weak field, it may be linearized writing the metric tensor as:

$$g_{\mu\nu} \simeq \eta_{\mu\nu} + h_{\mu\nu}$$

with $|h_{\mu\nu}| \ll 1$.
In vacuum, in the Lorenz Gauge and with the additional conditions of traceless and transversal gauge (TT), eq. (1) becomes:

$$\partial_\rho \partial^\rho h^{TT}_{\mu\nu} = 0.$$

The solution is a wave propagating in vacuum at the speed of light:[1]

$$h^{TT}_{\mu\nu} = \begin{pmatrix} 0 & 0 & 0 & 0 \\ 0 & h_+ & h_X & 0 \\ 0 & h_X & -h_+ & 0 \\ 0 & 0 & 0 & 0 \end{pmatrix}_{\mu\nu} \cos[\omega(t - z/c)]$$

[1] For a wave propagating along the z direction.

where h_+ and h_X are the gravitational wave polarizations. In presence of a source that has a typical dimension l, assuming that the observer is at distance $r \gg \lambda \gg l$, where λ is the emitted wave length, the solution is then:

$$h_{ij}^{TT}(t,z) \simeq \frac{2G}{c^4}\frac{\ddot{I}_{ij}^{TT}(t-r/c)}{r}$$

where I_{ij}^{TT} is the moment of inertia of the source projected in the transversal traceless gauge.

3 Detector

Virgo and LIGO detectors operate the same way but have some technicalities that make them slightly different. Fig. 1 displays schematically the Advanced Virgo detector, which is a laser interferometer with two perpendicular arms 3 km long. The laser ($\lambda = 1064\,\mathrm{nm}$) sends a beam to the Beam Splitter that divides it between the two arms. The two resulting beams travel through the arms and then are reflected from the final mirrors and may recombine. The detector output shows the interference between the two beams. When a gravitational wave occurs, it produces a perturbation of the arms' length and a consequent perturbation of the laser beams' interference. The output signal is the *strain* $h(t)$ which is the convolution between the detector pattern functions F_+ and F_X with the two polarization amplitudes h_+ and h_X. Typically, the strain is $\propto dL/L$ that is the differential variation of the light path; so, to make L as large as possible, it has been used a couple of mirrors (*Input Test Masses* in Fig. 1) that creates a Fabry-Pérot cavity in which the light is reflected many times. Even the *Power Recycling Mirror* is used to create a Fabry-Pérot cavity between itself and the *Beam Splitter* to recycle power. Finally, the *Input Mode Cleaner* is a triangular cavity that reduces the low-frequency noise while the *Squeezed Vacuum Injection* reduces high-frequency quantum noise.

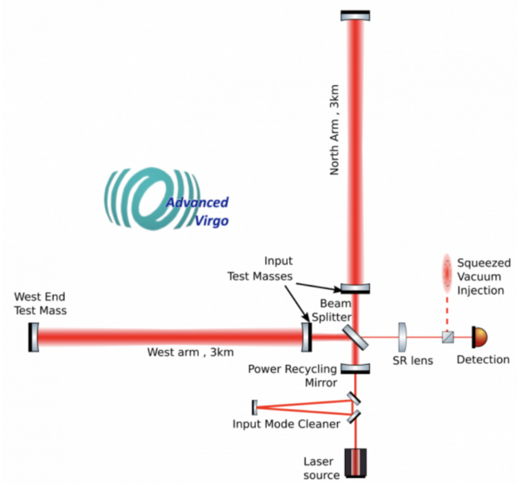

Figure 1: Advanced Virgo interferometer. Credits: The Virgo Collaboration

4 Data Analysis

The data are available on the Gravitational Wave Open Science Center (GWOSC) website [2].
The following analysis has been implemented using Python (Pandas, Astropy) and the Python packages for gravitational-wave astrophysics: *gwpy* and *pycbc*.
We have selected one-hour data around the GPS time $t_0 = 1186741861.5$ s. We have also done a data-quality check using the *gwpy* class *DataQualityFlag*.

4.1 Temporal analysis

Computing a plot of raw data, it's clear that in no detectors is possible to distinguish the gravitational wave (GW) signal from the noise, as we can see on the left of Fig. 2 . Even if it's not visible from the Fig. 2 because of the selection of a shorter interval range, we report that, in the Virgo data, a spike appears, but is found approximately ten minutes before the GPS time so it is not compatible with the GW signal.
Uncertainties in the time stamping of the data are

[2] www.gw-openscience.org

10 μs for LIGO and 20 μs for Virgo [1].
It has been applied a bandpass filter from 50 Hz to 300 Hz, but still it's possible to clearly recognize the strain growth only in the LIGO Livingstone, while for both the other detectors the signals remains deep in the noise, as we can see on the right of Fig. 2. Furthermore, from LIGO data we have removed lines due to the AC power grid (harmonics of 60 Hz in the US) applying the *pycbc* notch filter. For Virgo, this has been already considered when bandpassing (harmonics of 50 Hz in Europe).

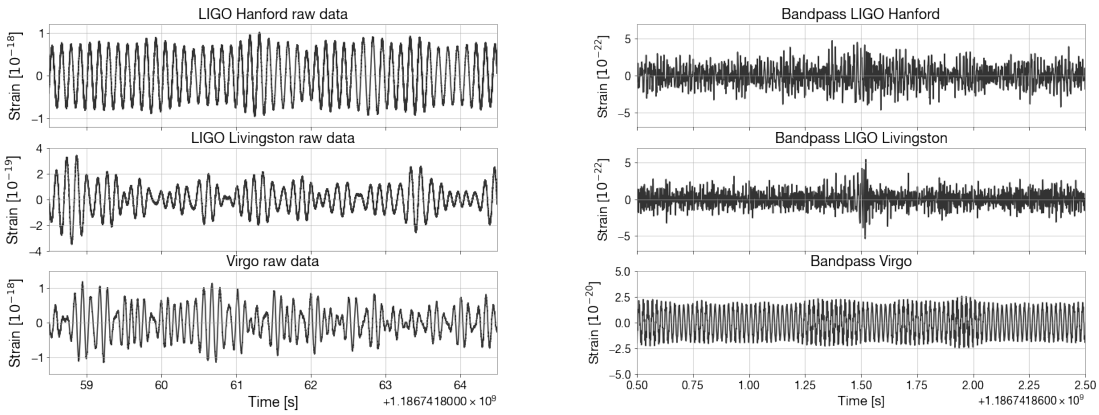

Figure 2: On the left, raw detectors data. On the right, data bandpassed from 50 Hz to 300 Hz.

4.2 Detector noise analysis

The noise is an example of a random process time series $x(t)$. All the noise sources set up a statistical ensemble that evolves according to a probability density function $p(t)$. The noise expectation value is:

$$\langle x \rangle = \int p(x) x \, dx$$

Even if the noise is almost never stationary (i.e. the noise properties are constant with time), by now we will assume it (see below).
Then, taking the time interval large enough, we can express $\langle x \rangle$ as a time average:

$$\langle x \rangle = \lim_{T\to\infty} \frac{1}{T} \int_{-T/2}^{T/2} x(t) \, dt.$$

To describe the power distribution in frequency that composes the signal, we introduce the Power Spectral Density (PSD) $S_x(f)$ of a time series $x(t)$. It is defined as the Fourier Transform of the two-point correlation function or, equivalently, as:

$$S_x(f) = \lim_{T\to\infty} \frac{2}{T} \left| \int_{-T/2}^{T/2} e^{-2\pi i f t} x(t) \, dt \right|^2 .$$

The data has been analyzed within a window of one hour around t_0.
Then, we have computed the Amplitude Spectral Density (ASD), which is the radical square of the PSD.
To have an initial look at the noise distribution in frequencies, it has been computed the mean ASD with the *median* method using the *asd* function from *pycbc*. We can immediately notice that, on average, Virgo is the noisiest detector.
To investigate the noise stationarity, we have computed the mean ASD over sub-intervals of ten seconds, selecting frequencies from 30 to 1000 Hz.
In Fig. 4, it's reported an histogram of the mean ASD ($\overline{ASD}$) occurrences for each detector. The relative deviation from the mean of the $\overline{ASD}$ values is about 2% for Hanford, 3% for Livingston and 10% for Virgo, so the noise could be considered stationary with good approximation.
Furthermore, we have computed a deeper analysis of the noise time evolution as a function of frequency. The Time Series has been divided into sub-intervals 4 seconds long; then, for each sub-interval, has been computed the ASD. Now we want to investigate how each frequency evolves with time. For each ASD function, we have divided the frequency range into sub-intervals of 1 Hz, then, for each one, we have computed the mean ASD value. We have realized a 2D histogram (Fig. 5) where is plotted on the z-axis (through the color scale) the ASD mean value for each sub-interval as a function of frequency. The color scale has been set equal for all the detectors

to better appreciate the ASD differences between them.

This deeper noise investigation is another control for stationarity: in fact, for all frequencies range, we don't see appreciable noise ASD variation over time. However, as we can see, there are some frequencies in which the noise maintains high ASD values during all the data set. In particular, low frequencies (under about $20 - 30\,\mathrm{Hz}$) present a higher noise in all detectors. Above 60 Hz, we note in Virgo some noise peaks, i.e. at 300 Hz or 600 Hz, that are not instead important for the two LIGO. Livingston presents a visible peak at 500 Hz that is fainter both in Hanford and Virgo. For Hanford, we note a noise peak also at 1 kHz, which is not rather important for the others. Furthermore, we can note that, between about 20 and 30 minutes, there is in Virgo a horizontal darker line, which means that the noise has had a quick temporary increase, especially between 10 and 50 Hz.

Therefore, the better sensibility results for frequencies over about 100 Hz and it is greater in the two LIGO compared to Virgo.

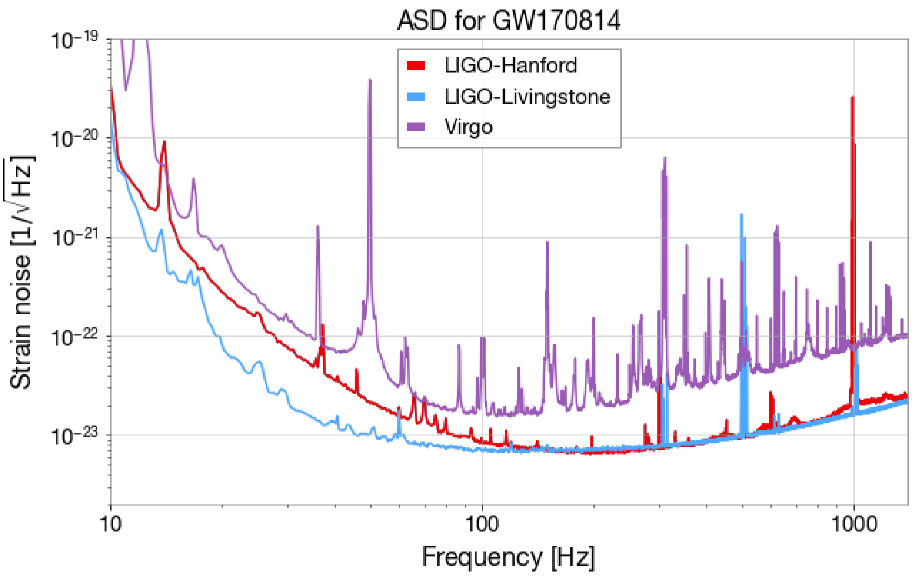

Figure 3: ASD for time intervals 4 seconds long.

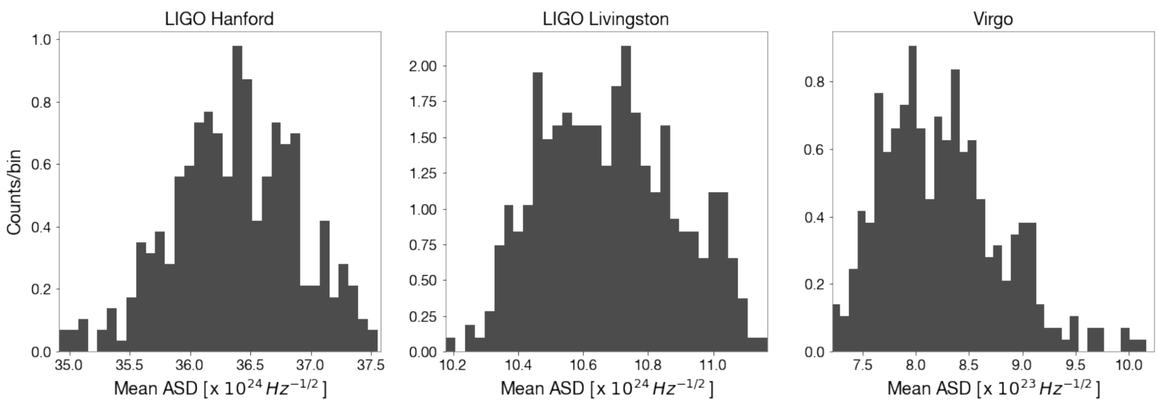

Figure 4: Mean ASD occurances for time interval of 10 seconds considering 30-1000 Hz frequency interval. Bin is set equal to 0.08 for Hanford, to 0.03 for Livingston and to 0.08 for Virgo. All the histograms are normalized.

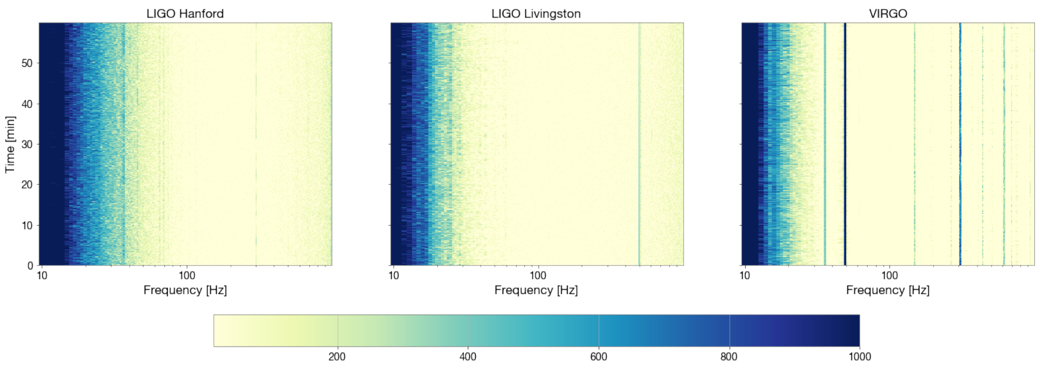

Figure 5: ASD time evolution as a function of frequency.

4.3 Optimal detection filter

The search for a gravitational signal has been based on a Hypothesis Test. Given the detector Time Series $s(t)$, we want to compare two different hypothesis:

- H_0: $s(t) = n(t)$, "no signal"
- H_1: $s(t) = n(t) + h(t, \Theta)$, "signal"

where $n(t)$ is the noise and $h(t, \Theta)$ is an hypothetical wave form that depends on a set of parameters Θ, that is in general called template.
A signal can only be detected if the null hypothesis is sufficiently disfavored relative to the signal hypothesis.
We define the *likelihood ratio* as: [3]

$$\Lambda(H_1|s) = \frac{p(s|H_1)}{p(s|H_0)}.$$

Assuming Gaussian noise, we have that:

$$\begin{aligned} P(s|H_0) &= P_n[s] \ \propto \ e^{-(s,s)/2} \\ P(s|H_1) &= P_n[s-h] \ \propto \ e^{-(s-h,s-h)/2} \\ \Rightarrow \ \ \Lambda(H_1|s) &= e^{(s,h)}e^{-(h,h)/2} \end{aligned}$$

where we have defined the product (a,b) as:

$$(a,b) = 4Re\int_0^\infty \frac{\tilde{a}(f)\tilde{b}^*(f)}{S_n(f)}\,df,$$

a quantity also known as *matched filter* that gives a noise-weighted correlation between signal and template. Then, shifting the template, we can find the time for which the correlation has a maximum. We therefore have:

$$\begin{aligned} \Lambda(H_1|s) &= e^{(s,h)}e^{-(h,h)/2} \\ \Rightarrow \quad \log(\Lambda(H_1|s)) &= (s,h) - \frac{1}{2}(h,h) \end{aligned}$$

The Θ parameters are, in general, 15: 8 are intrinsic (the two Black Holes masses m_1 and m_2 and their spin $\vec{s_1}$ and $\vec{s_2}$) and 7 extrinsic (i.e. depending on the observer position with respect to the system).
The extrinsic parameters can be obtained algebraically maximizing Λ over parameters. Here we have focused on the estimate of intrinsic parameters, that can be done using a computational approach in Python.
First of all, It has been assumed that $\vec{s_1}$ and $\vec{s_2}$ are null (as stated in [1]).
The used method is based on exploring a grid of masses defined by a mass step $dm = 0.1$ [4] sweeping in the mass range of [20, 40], using the exchange symmetry between the two masses.
Previously, the data has been downsampled at 2048 Hz and high-passed at 15 Hz, using the function *resample_to_delta_t* and *highpass*; then two seconds at both the edges of the temporal series have been cropped to avoid edges effects due to the resampling. After the data cleaning up, we have computed the Power Spectral Density (PSD) over 4 seconds data using the Welch method. Then, with the data and the PSD, we have derived the *matched_filter()* function using a grid of masses generating a template bank using the approximant "SEOBNRv4_opt". The function returns the SNR for each template, defined as:

$$\text{SNR} = \frac{(s,h)}{\sqrt{(h,h)}}.$$

It's possible to demonstrate that maximizing the SNR, also the *likelihood ratio* will be maximized. This way, it's possible to find the template with

[3] In the following, it is used s instead of $s(t)$ to simplify notation
[4] All masses are measured in solar unit: 1 $M_\odot \simeq 1.989 \times 10^{30}$ Kg.

the maximum peak: this corresponds to the wave form with the best masses estimate, reported in Tab. 1 with also the estimate of the time at which detectors register the event (corresponding to the time of the SNR peak). The error over masses is set equal to one step of the search grid.
On the left of Fig. 6, it's plotted the SNR with the maximum peak value for each detector.
The best template has been time-shifted to the peak time and then it has been scaled in amplitude and phase to the peak value. On the right of Fig. 6, are shown for all detectors the proposed template overlapped to data, which have been both previously whiten (i.e. normalized to the PSD).
In Fig. 7 is shown the spectrogram for LIGO Hanford: in the upper panel are plotted the original data while the second panel shows the plot of the proposed template subtracted to data. This is a quick check of the template goodness, since from the second panel, having subtracted the template, we can not appreciate anything but noise.

Detector	m_1 $[M_\odot]$	m_2 $[M_\odot]$	t_{peak} (+1186741861.0 s)
LIGO Hanford	28.1(1)	30.9(1)	0.53223(1)
LIGO Livingston	29.5(1)	31.2(1)	0.52344(1)
Virgo	25.4(1)	26.0(1)	0.63086(2)

Table 1: Masses estimate and detection time.

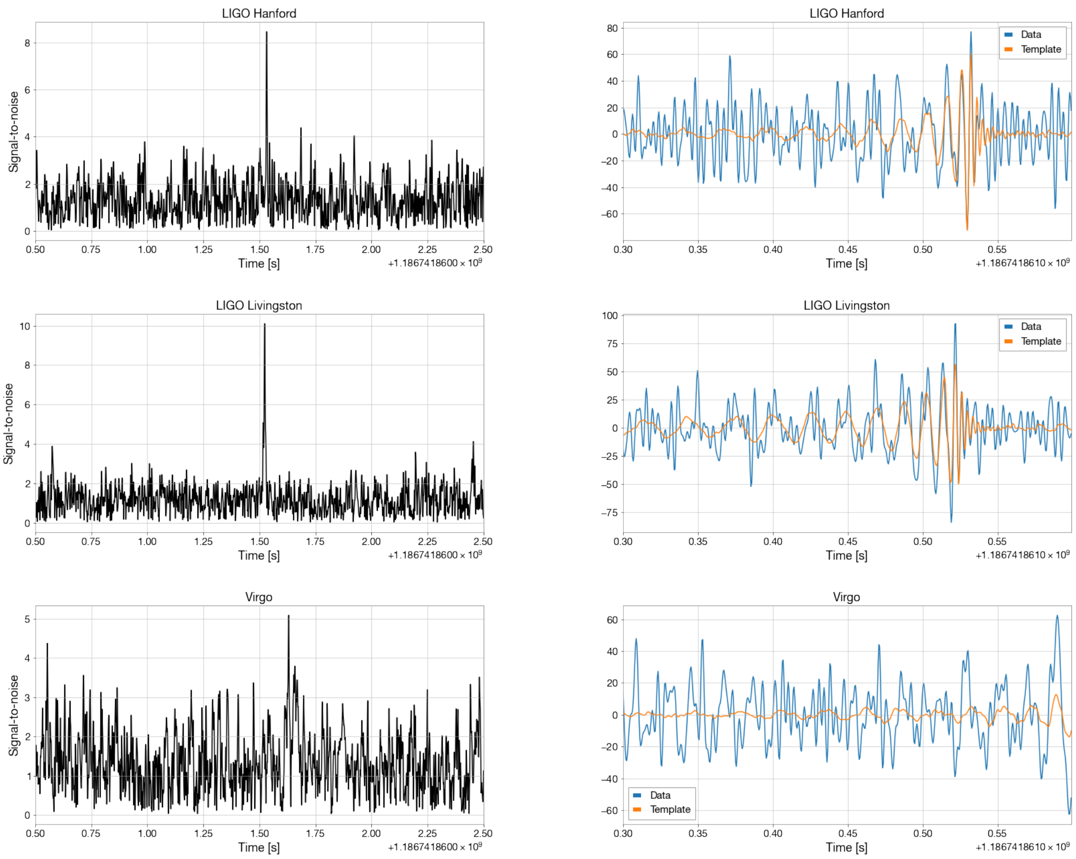

Figure 6: On the left, we see for each detector the SNR computed with the template with the higher SNR peak. On the left, we can see the overlap between the best template and the data.

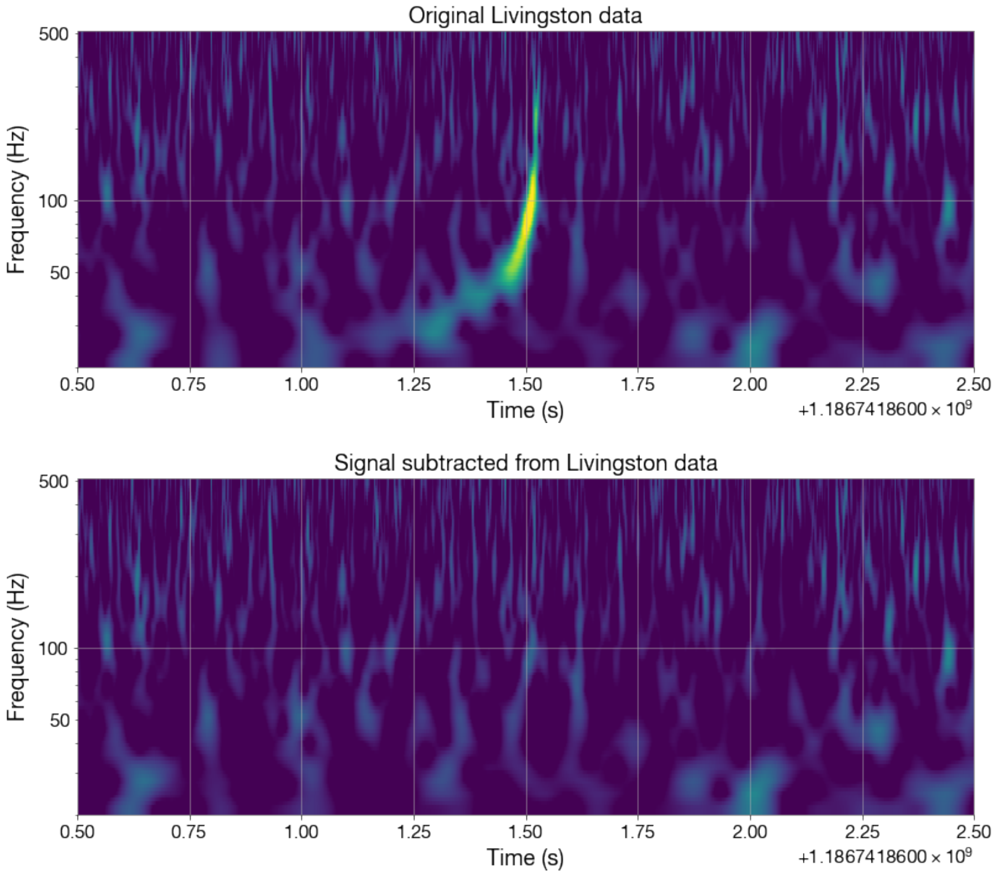

Figure 7: Spectrogram for the Livingston data (up panel) and for the Livingston best template subtracted from data (down panel).

5 Conclusions

We have been able to study the noise and to give a template for each data set for both LIGO detectors. For Virgo, we did not successfully find a proper template. For each detector, we have managed to estimate the BHs masses that are compatible with the masses in *Abbot et al.* [1], that are $m_1 = 25.3^{+2.8}_{-4.2} M_\odot$ and $m_2 = 30.5^{+5.7}_{-3.0} M_\odot$.
The signal time occurrence is consistent with the *Abbott al.* [1] regarding the order of detection, while the delay of detection of Hanford and Virgo is consistent only for Hanford, maybe due to the wrong template choice in Virgo. In fact, we have that $t_H - t_L \simeq 8.8$ ms and $t_V - t_L \simeq 107$ ms, while in [1] the delays are ~ 8 ms and ~ 14 ms.

References

[1] B. P. Abbott et al., GW170814: A Three-Detector Observation of Gravitational Waves from a Binary Black Hole Coalescence, Physical Review Letters PRL 119, 141101 (2017).

[2] B. P. Abbott et al., A guide to LIGO-Virgo detector noise and extraction of transient gravitational-wave signals, arXiv: 1908.11170v3 [gr-qc] 10 Feb 2020